First-principles analysis of the Raman spectrum of vitreous silica: comparison with the vibrational density of states

2003 J. Phys.: Condens. Matter 15 S1547

(http://iopscience.iop.org/0953-8984/15/16/304)

INSTITUTE OF PHYSICS PUBLISHING JOURNAL OF PHYSICS: CONDENSED MATTER

J. Phys.: Condens. Matter **15** (2003) S1547–S1552 PII: S0953-8984(03)54806-8

First-principles analysis of the Raman spectrum of vitreous silica: comparison with the vibrational density of states

P Umari and Alfredo Pasquarello

Institut de Théorie des Phénomènes Physiques (ITP), Ecole Polytechnique Fédérale de Lausanne (EPFL), CH-1015 Lausanne, Switzerland
and
Institut Romand de Recherche Numérique en Physique des Matériaux (IRRMA), CH-1015 Lausanne, Switzerland

E-mail: Paolo.Umari@epfl.ch and Alfredo.Pasquarello@epfl.ch

Received 16 October 2002
Published 14 April 2003
Online at stacks.iop.org/JPhysCM/15/S1547

Abstract

The HH and HV Raman spectra of vitreous silica are calculated from first principles for a model structure consisting of a disordered network of corner-sharing tetrahedra, for which the vibrational properties were obtained previously. We analyse the contribution of specific atomic motions to the Raman spectra and perform a detailed comparison with respect to the vibrational density of states. We find that the HV spectrum closely resembles the vibrational density of states. By comparison, the HH spectrum shows significant differences and arises almost exclusively from oxygen vibrations.

1. Introduction

Raman scattering spectroscopy is routinely used as a powerful experimental tool for the investigation of materials and, in particular, of disordered solids [1]. It is common practice to interpret the Raman spectra of disordered materials in terms of the vibrational density of states, because Raman cross-sections are not, in general, readily available. In fact, the analysis and the interpretation of Raman intensities are not straightforward and require accurate theoretical modelling.

For crystalline solids, first-principles methods have proved very successful in reproducing Raman cross-sections [2–4]. However, the application of these approaches to calculate the Raman spectra of disordered materials has long been prevented by the computational effort required for treating systems of large size.

Among the disordered materials, vitreous silica is of particular interest, not only because of its prominent technological applications, but also because it represents a prototypical example of a disordered network-forming system. This material has been extensively characterized via

vibrational spectroscopies, including inelastic neutron scattering [5], infrared absorption [6], and Raman scattering [7]. While the former two spectroscopies have successfully been modelled within first-principles schemes [8–10], the detailed interpretation of Raman spectra still relies on simplified theoretical approaches, such as the bond polarizability model [11].

We here compare the vibrational density of states and the Raman spectra, both calculated from first principles, for the *same* model structure of vitreous silica, in order to highlight the effect of the Raman cross-sections. We use a model of vitreous silica consisting of corner-sharing tetrahedra [12], for which the vibrational properties, and in particular the vibrational density of states, were obtained previously [8, 10]. We calculate the HH- and HV-polarized Raman spectra for our model structure using a linear response method. We extend the comparison between the vibrational density of states and the Raman spectra by distinguishing the contributions from oxygen and silicon vibrations. Our analysis shows that the HH spectrum is dominated by oxygen vibrations, while the HV spectrum more closely resembles the vibrational density of states.

This paper is organized as follows. In section 2, we give a brief outline of the theoretical formulation used for describing the Raman spectra of disordered materials. In section 3, we show the calculated HH and HV spectra for vitreous silica. These spectra are then analysed in terms of contributions from specific vibrational motions.

2. Theoretical formulation

In the Raman scattering process, photons are inelastically scattered by vibrational excitations. The calculation of the first-order Raman intensities for a disordered material relies on the availability of three main ingredients: the model structure, its vibrational frequencies and eigenmodes, and the derivatives of the polarizability tensor with respect to the individual atomic displacements.

For a model system, the vibrational frequencies ω_k and their associated eigenmodes $\boldsymbol{v}_\alpha^k$ are found by solving the set of linear equations:

$$D_{\alpha i,\beta j} v_{\beta j}^k = \omega_k^2 v_{\alpha i}^k, \tag{1}$$

where $\mathbf{D}$ is the dynamical matrix, and where the Greek and Latin indices run over the atoms in the primitive cell and the three Cartesian directions, respectively. The dynamical matrix $\mathbf{D}$ is defined by

$$D_{\alpha i,\beta j} = \frac{1}{\sqrt{M_\alpha M_\beta}} \frac{\partial^2 E_{\mathrm{tot}}}{\partial r_{\alpha i}\, \partial r_{\beta j}}, \tag{2}$$

where E_{tot} is the total energy of the system, and $\boldsymbol{r}_\alpha$ and M_α are the position and the atomic mass of atom α. Diagonalization of the dynamical matrix $\mathbf{D}$ gives the vibrational frequencies ω_k and the normalized eigenmodes $\boldsymbol{v}_\alpha^k$. The Raman susceptibility tensors $\boldsymbol{\alpha}^k$ are then given for each mode k by

$$\alpha_{ij}^k = \sqrt{\Omega} \sum_{\alpha l} \frac{\partial \chi_{ij}}{\partial r_{\alpha l}} \frac{v_{\alpha l}^n}{\sqrt{M_\alpha}}, \tag{3}$$

where $\boldsymbol{\chi}$ is the electric polarizability tensor, and Ω the volume of the primitive cell.

In experimental set-ups, it is customary to record the Raman spectra in the HH and the HV configurations, in which the polarization of the outgoing photons is parallel and orthogonal to the ingoing photon polarization, respectively [13]. Using the isotropy of disordered solids, we express the contributions of the kth mode to the HH and HV Raman spectra as [1]

$$I_{\mathrm{HH}}^k = a_k^2 + \tfrac{4}{45} b_k^2, \tag{4}$$

$$I_{\mathrm{HV}}^k = \tfrac{3}{45} b_k^2, \tag{5}$$

where a^k and b^k are obtained from

$$\begin{aligned} a_k &= \tfrac{1}{3}(\alpha^k_{11} + \alpha^k_{22} + \alpha^k_{33}) \\ b^2_k &= \tfrac{1}{2}[(\alpha^k_{11} - \alpha^k_{22})^2 + (\alpha^k_{11} - \alpha^k_{33})^2 + (\alpha^k_{22} - \alpha^k_{33})^2] + 3[(\alpha^k_{12})^2 + (\alpha^k_{13})^2 + (\alpha^k_{23})^2]. \end{aligned} \tag{6}$$

Focusing on the Stokes process, in which a vibrational excitation is created by an incoming photon, we express the total power cross-section as (in esu units)

$$I^P_{\mathrm{HH,HV}}(\omega) = 4\pi \sum_k \frac{(\omega_\mathrm{L} - \omega_k)^4 V}{c^4} I^k_{\mathrm{HH,HV}} \frac{\hbar}{2\omega_k}[n(\omega_k) + 1]\delta(\omega - \omega_k), \tag{7}$$

where V is the volume of the scattering sample, w_L the frequency of the incoming photon, c the speed of light, and $n(\omega)$ the boson factor:

$$n(\omega) = \frac{1}{\exp(\hbar\omega/k_\mathrm{B}T) - 1}. \tag{8}$$

In this work, we give the Raman intensities using the following reduced expression:

$$I^P_\mathrm{R}(\omega) = \omega(\omega_\mathrm{L} - \omega)^{-4}(n(\omega) + 1)^{-1} I^P(\omega). \tag{9}$$

3. Analysis of Raman spectra

We used a model structure of vitreous silica, which was previously obtained by first-principles molecular dynamics [12]. The model adopted [12] contains 72 atoms in a periodically repeated cubic cell, at the experimental density (2.20 g cm^{-2}). The structure consists of a network of corner-sharing tetrahedra with no coordination defects. We described the electronic structure within density functional theory using the local density approximation [14] for the exchange and correlation energy. Only valence wavefunctions were treated explicitly and the interaction between valence and core electrons was modelled by a norm-conserving pseudopotential for Si and an ultrasoft one [15] for O. The wavefunctions and the density are described by plane-wave basis sets defined by cut-off energies of 24 and 200 Ryd, respectively [16, 17]. The dynamical matrix of this model structure was obtained previously by the finite-difference method [8, 10]. The inelastic neutron spectrum [8, 10] and the infrared absorption spectrum [9] were calculated on the basis of the resulting vibrational properties, and they were found to be in accord with experiment.

To obtain the Raman spectra, we calculated by the finite-difference method the derivatives of the polarizability tensor with respect to atomic displacements $\partial\chi_{ij}/\partial r_{\alpha l}$. The polarizability tensors χ_{ij} were calculated from first principles using a linear response method [18]. Every atom was displaced from its equilibrium position by ± 0.07 Bohr, along each of the three Cartesian directions. Our confidence in the reliability of a first-principles description of Raman intensities for vitreous silica stems from the good agreement with experiment obtained for crystalline forms of tetrahedrally bonded SiO_2 [4].

In figure 1, we report the calculated HH and HV reduced Raman spectra, together with the vibrational density of states [10]. With respect to experiment [7], the calculated Raman spectra show fair agreement as regards the location of the principal peaks and the distribution of their intensities. The ratios between the intensities in the HH and HV spectra also agree well with the experimental measurements. An important difference between theory and experiment occurs in the HH spectrum for the intensity of the defect line D_2 at about 610 cm^{-1}, which results from a high concentration of threefold rings in our model structure [11, 19]. This difference with respect to experiment does not invalidate the significance of a comparison between the Raman spectra and the vibrational density of states, since both refer to the same model structure. We

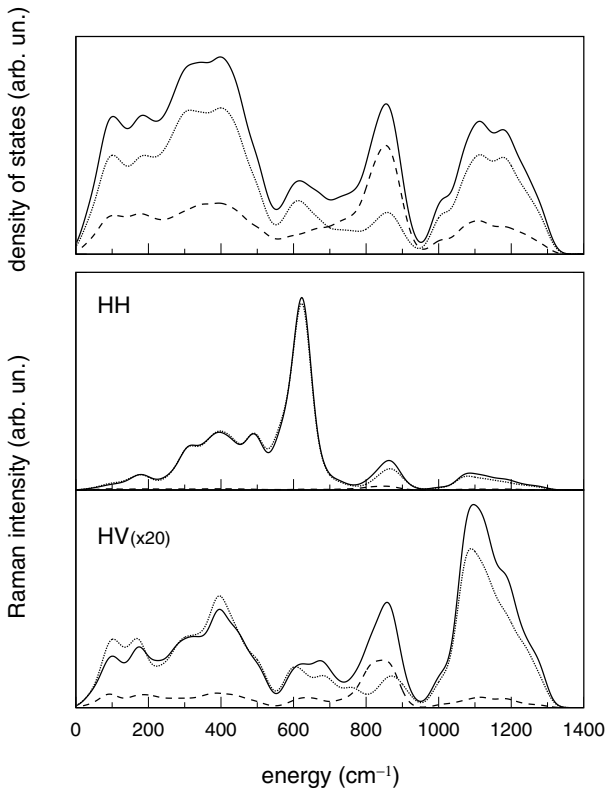

Figure 1. The vibrational density of states [10] and HH and HV reduced Raman spectra as calculated for the same model structure of vitreous silica (solid). Contributions from oxygen (dotted) and silicon (dashed) vibrations are given.

will present elsewhere the structural information concerning the ring statistics in vitreous silica which can be derived from a close comparison between theory and experiment [18].

The reduced HH Raman spectrum appears significantly different from the vibrational density of states. In part, this results from the intensity of the D_2 line, which does not find a counterpart in the vibrational density of states. The D_1 line associated with fourfold rings and occurring at about 500 cm^{-1} also modifies the HH spectrum with respect to the vibrational density of states. In the lowest part of the HH spectrum, up to 200 cm^{-1}, the Raman intensity appears suppressed with respect to the vibrational density of states. A resemblance between the HH spectrum and the vibrational density of states is only recognized for frequencies higher than $\sim$750 cm^{-1}. In contrast, the HV reduced Raman spectrum closely resembles the vibrational density of states over the whole range of the spectrum. This accord relates to both the location of the main peaks and their relative intensities. With respect to the vibrational density of states, only a slight enhancement of the high-frequency peak ($>$1000 cm^{-1}) is found in the HV spectrum. The same effect is observed, to a lesser extent, for the peak at $\sim$800 cm^{-1}.

We extend the comparison between the Raman spectra and the vibrational density of states further by analysing the contributions from oxygen and silicon vibrations. The decomposition of the vibrational density of states into partial densities associated with specific atoms is well defined [10]. For the Raman spectra, we obtain partial spectra by considering only silicon or oxygen atoms in the sum over α in equation (3). Unlike the case for the vibrational density of states, the sum of the partial Raman spectra does not recover the full spectrum,

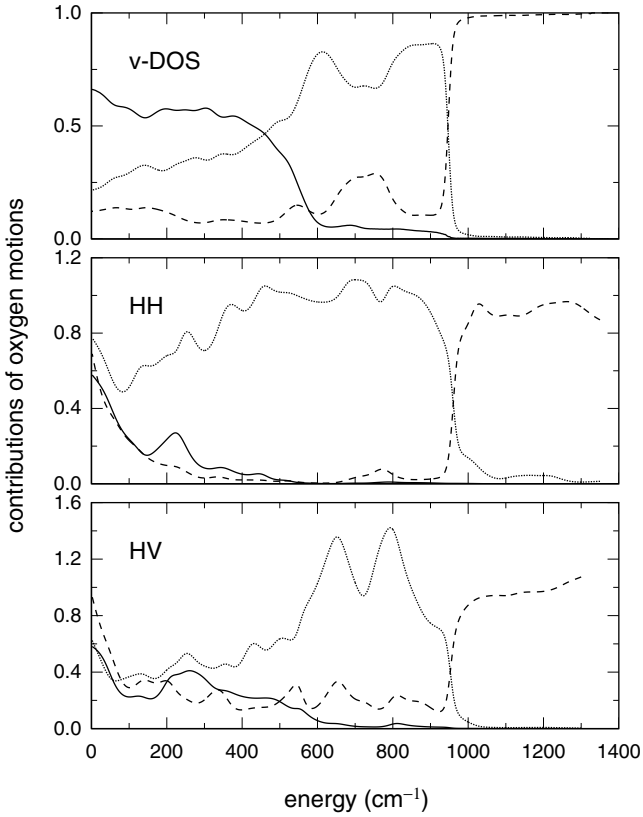

Figure 2. Contributions to the vibrational density of states [10], and to the HH and HV Raman spectra from oxygen vibrations decomposed according to rocking (solid), bending (dotted), and stretching (dashed) vibrations. The contributions are expressed as ratios with respect to the total oxygen contribution.

because of interference terms. However, this decomposition still gives a measure of the relative contributions from oxygen and silicon vibrations to the Raman intensities.

As shown in figure 1, the HH spectrum is dominated by oxygen vibrations, the silicon contribution being essentially negligible. The decomposition of the HV Raman spectrum further supports the resemblance with the vibrational density of states. The ratio between oxygen and silicon contributions appears only slightly higher in the HV spectrum than in the vibrational density of states.

Because of the prominent contribution of oxygen vibrations to the Raman spectra, we further decomposed this contribution according to three directions which characterize the local environment of each oxygen atom [20]. Considering the plane containing the Si atoms to which a given O atom is bonded, we defined the three directions as in [10]. We took the first direction orthogonal to the Si–O–Si plane (rocking), the second one along the bisector of the Si–O–Si angle (bending), and the third one orthogonal to the two previous ones (stretching). The decomposition was carried out by projecting the eigenmodes $\boldsymbol{v}_\alpha^k$ on these directions prior to the calculation of the Raman tensors given in equation (3).

In figure 2, the oxygen contributions to rocking, bending, and stretching vibrations are expressed as ratios with respect to the total oxygen contribution. The decomposition of the vibrational density of states is from [10]. In all the decompositions in figure 2, the

high-frequency part of the spectra ($\gtrsim$1000 cm^{-1}) almost exclusively results from stretching vibrations. As far as the HH spectrum is concerned, the decomposition indicates that the bending motions dominate the rest of the spectrum. In particular, the contribution of rocking vibrations is suppressed with respect to their weight in the vibrational density of states. The decomposition of the HV Raman spectrum again shows the closest resemblance with the vibrational density of states. The rocking component is found to be smaller than in the vibrational density of states, but larger than in the HH Raman spectrum.

4. Conclusions

The HH and HV Raman spectra were calculated from first principles for a model structure of vitreous silica and compared with the vibrational density of states for the *same* model structure. We found that the HV Raman spectrum closely resembles the vibrational density of states. Our analysis in terms of contributions from specific vibrations shows that the resemblance also holds at this more detailed level of comparison. This resemblance supports the practice of obtaining an estimate of the vibrational density of states from a measurement of the HV Raman spectrum. On the other hand, the HH Raman spectrum shows significant differences with respect to the vibrational density of states. These differences also show up in the decomposition in terms of contributions from specific atomic vibrations. In fact, the HH Raman spectrum almost exclusively arises from oxygen vibrations, with dominating bending and stretching motions below and above $\sim$1000 cm^{-1}, respectively.

Acknowledgments

We acknowledge support from the Swiss National Science Foundation (grant nos 21-55450.98 and 620-57850.99) and the Swiss Centre for Scientific Computing.

References

[1] Cardona M (ed) 1983 *Light Scattering in Solids* vol 1, 2nd edn (Berlin: Springer)
Cardona M and Güntherodt G (ed) 1982 *Light Scattering in Solids* vol 2 (Berlin: Springer)
[2] Baroni S and Resta R 1986 *Phys. Rev.* B **33** 5969
[3] Windl W, Pavone P, Karck K, Schütt O, Strauch D, Giannozzi P and Baroni S 1993 *Phys. Rev.* B **48** 3164
[4] Umari P, Pasquarello A and Dal Corso A 2001 *Phys. Rev.* B **63** 94305
[5] Carpenter M J and Price D L 1985 *Phys. Rev. Lett.* **54** 441
[6] Kirk C T 1988 *Phys. Rev.* B **38** 1255
[7] Galeener F L and Lucovsky G 1976 *Phys. Rev. Lett.* **37** 1474
[8] Sarnthein J, Pasquarello A and Car R 1997 *Science* **275** 1925
[9] Pasquarello A and Car R 1997 *Phys. Rev. Lett.* **70** 1766
[10] Pasquarello A, Sarnthein J and Car R 1998 *Phys. Rev. Lett.* **57** 14133
[11] Umari P and Pasquarello A 2002 *Physica* B **316/317** 572
[12] Sarnthein J, Pasquarello A and Car R 1995 *Phys. Rev. Lett.* **74** 4682
Sarnthein J, Pasquarello A and Car R 1995 *Phys. Rev.* B **52** 12690
[13] Brüesch P 1986 *Phonons: Theory and Experiments* vol 2 (Berlin: Springer)
[14] Perdew J P and Zunger A 1981 *Phys. Rev.* B **23** 5048
[15] Vanderbilt D 1990 *Phys. Rev.* B **41** 7892
[16] Pasquarello A, Laasonen K, Car R, Lee C and Vanderbilt D 1992 *Phys. Rev. Lett.* **69** 1982
[17] Laasonen K, Pasquarello A, Car R, Lee C and Vanderbilt D 1993 *Phys. Rev.* B **47** 10142
[18] Umari P, Gonze X and Pasquarello A 2002 unpublished
[19] Pasquarello A and Car R 1998 *Phys. Rev. Lett.* **80** 5145
[20] Bell R J, Dean P and Hibbins-Butler D C 1971 *J. Phys. C: Solid State Phys.* **4** 1241
Bell R J and Hibbins-Butler 1975 *J. Phys. C: Solid State Phys.* **8** 787